Eguchi, Kei; Kuwahara, Kyoka; Ishibashi, Takaaki

Article

Analysis of an LED lighting circuit using a hybrid buck-boost converter with high gain

Energy Reports

Provided in Cooperation with:
Elsevier

Suggested Citation: Eguchi, Kei; Kuwahara, Kyoka; Ishibashi, Takaaki (2020) : Analysis of an LED lighting circuit using a hybrid buck-boost converter with high gain, Energy Reports, ISSN 2352-4847, Elsevier, Amsterdam, Vol. 6, Iss. 2, pp. 250-256, https://doi.org/10.1016/j.egyr.2019.11.070

This Version is available at:
https://hdl.handle.net/10419/243886

Available online at www.sciencedirect.com
ScienceDirect
Energy Reports 6 (2020) 250–256
www.elsevier.com/locate/egyr

The 6th International Conference on Power and Energy Systems Engineering (CPESE 2019), September 20–23, 2019, Okinawa, Japan

Analysis of an LED lighting circuit using a hybrid buck–boost converter with high gain

Kei Eguchi[a,*], Kyoka Kuwahara[a], Takaaki Ishibashi[b]

[a] *Department of Information Electronics, Fukuoka Institute of Technology, 3-30-1 Wajirohigashi, Higashi-ku, Fukuoka, 811-0295, Japan*
[b] *Department of Electronics Engineering and Computer Science, National Institute of Technology, Kumamoto College, 2659-2 Suya, Koushi-shi, Kumamoto, 861-1102, Japan*

Received 2 October 2019; accepted 22 November 2019

Abstract

In this paper, a hybrid buck–boost dc–dc converter and its analysis method are presented for LED lighting applications. Unlike existing LED driver circuits, the proposed driver circuit has a hybrid structure which consists of a buck–boost converter and a switched-capacitor (SC) step-up converter with flying capacitors. The features of the proposed driver are as follows: 1. High voltage gain provided by cascading two dc–dc converters, 2. Flexible LED current control using step-up/step-down conversion, and 3. Small volume offered by a single inductor structure. Concerning the proposed driver circuit, a simple equivalent circuit is derived by theoretical analysis. Furthermore, the characteristics of the proposed converter are revealed by simulation program with integrated circuit emphasis (SPICE) simulations and breadboard experiments. The results of simulation and experiment demonstrate the feasibility of the proposed driver circuit. The proposed driver circuit can achieve about 89% efficiency and −10 V output when the output load is 400 mW.

Peer-review under responsibility of the scientific committee of the 6th International Conference on Power and Energy Systems Engineering (CPESE 2019).

Keywords: Hybrid DC–DC converters; Buck–boost converters; LED lighting applications; Step-up converters; Switched-capacitor techniques

1. Introduction

In LED (Light Emitting Diodes) lighting applications, an LED driver circuit is necessary to transform an input voltage to a high voltage for emitting light, because long strings of LEDs are commonly used to provide easy current control of LEDs. In past studies, three types of LED driver circuits have been proposed: inductor-based converter topology, capacitor-based converter topology, and hybrid converter topology combined with some power converters. The inductor-based converter topologies, such as buck–boost type [1], boost type [2], LLC type [3], can provide controllability of conversion ratios and simple circuit configuration. However, the inductor-based converter

* Corresponding author.
E-mail address: eguti@fit.ac.jp (K. Eguchi).

https://doi.org/10.1016/j.egyr.2019.11.070

Peer-review under responsibility of the scientific committee of the 6th International Conference on Power and Energy Systems Engineering (CPESE 2019).

topology is difficult to achieve high voltage gain, because there is a limitation to control the duty cycle in actual dc–dc converters. Unlike the inductor-based converter topologies, the capacitor-based converter topologies, such as Fibonacci type [4], Dickson type [5] and [6], do not use any magnetic components. Therefore, the capacitor-based converter topology can offer small size, light weight, and less electromagnetic interference (EMI). However, the capacitor-based converter topology suffers from poor regulation, because the conversion ratio is predetermined by the converter topology.

To solve above-mentioned problems, some LED drivers with hybrid topologies have been proposed, such as the LED driver combined with a boost converter and an LLC converter [7], LED driver combined with the Fibonacci converter and a buck–boost converter [8]. However, Ma's LED driver requires several magnetic components, although high voltage gain can be achieved. On the other hand, McRae's LED driver can realize flexible conversion ratio by using only one inductor. However, it provides the output voltage by adding the output of the Fibonacci converter to that of the buck–boost converter. Therefore, in order to offer a high stepped-up voltage, the size of the Fibonacci converter becomes bulky.

In this paper, a hybrid buck–boost dc–dc converter and its analysis method are presented. Unlike existing LED driver circuits, the proposed LED driver circuit has a hybrid structure by combining a buck–boost dc–dc converter with a switched-capacitor (SC) step-up converter with flying capacitors. Therefore, by cascading two-types of dc–dc converters, the proposed driver can provide high voltage gain, flexible LED current control, and small volume with a single inductor structure. The characteristics of the proposed hybrid converter are clarified by theoretical analysis, SPICE simulations, and breadboard experiments.

2. Circuit configuration

2.1. LED driver circuit using traditional buck–boost converter

Fig. 1 illustrates the LED driver circuit using a traditional buck–boost converter. The LED driver circuit using buck–boost converters drives the cathode terminal of LED strings to illuminate LEDs. The output voltage V_{om} of the traditional buck–boost converter is given by

$$V_{om} = -\frac{d}{(1-d)} \times V_{in}, \tag{1}$$

where D is a duty cycle. By controlling the parameter D, the current control of LEDs can be achieved. Although the output voltage of Eq. (1) is proportional to the parameter D, there is a limitation in actual dc–dc converters. So, it is difficult to achieve high voltage gain in the traditional buck–boost converter. To avoid the complexity of the current control of LEDs, long strings of LEDs are commonly used in LED devices. Therefore, it is necessary to give a larger voltage to the LED.

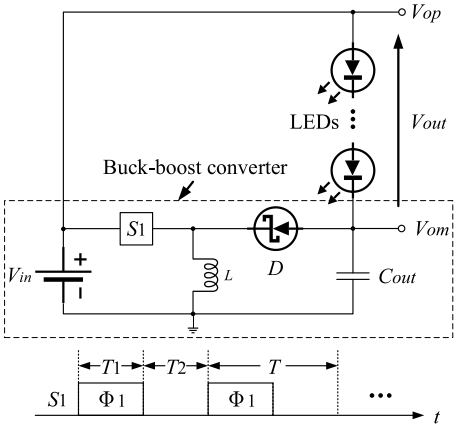

Fig. 1. Circuit configuration of the conventional LED driver circuit.

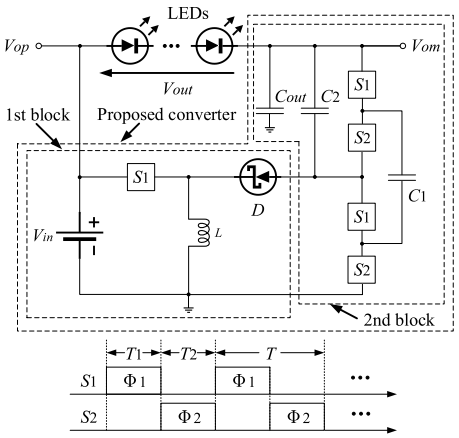

Fig. 2. Circuit configuration of the conventional LED driver circuit.

2.2. LED driver circuit using proposed hybrid buck–boost converter with high gain

Fig. 2 illustrates the circuit configuration of the proposed LED deriver circuit using the proposed hybrid buck–boost converter. Unlike the traditional buck–boost converter, the proposed hybrid buck–boost converter consists of a buck–boost converter and a switched-capacitor (SC) step-up converter with a flying capacitor. In Fig. 2, the current control of LEDs is achieved by the 1st block, and the high voltage gain is realized by cascade-connecting the 1st block and the 2nd block. When the switch S_2 is on, the capacitor C_1 is charged by the output voltage of the 1st converter block. On the other hand, when the switch S_1 is on, the capacitor C_2 is charged by the capacitor C_1. In this timing, the capacitor C_2 is connected in series to the output terminal of the 1st converter block. Therefore, the proposed converter provides the following output voltage:

$$V_{om} = -\frac{2d}{(1-d)} \times V_{in}. \tag{2}$$

As Eq. (2) shows, the voltage gain of the proposed hybrid converter is 2 times of that of the traditional buck–boost converter. The detail theoretical analysis of the proposed hybrid converter will be demonstrated in the next section.

3. Theoretical analysis

To simplify the theoretical analysis, the equivalent circuit of the proposed hybrid converter is obtained by assuming the conditions that 1. Parasitic elements are small and 2. Time constant is much larger the period of clock pulses. The theoretical analysis is divided into two parts: Analysis of the 1st block and the 2nd block.

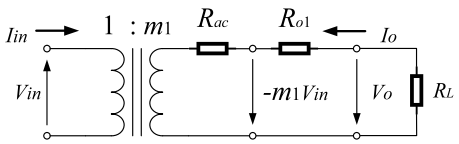

Fig. 3. Equivalent circuit of the 1st block.

First, the equivalent circuit of the 1st block is obtained by using the four-terminal equivalent model shown in Fig. 3 [9,10], where R_{o1} is the internal resistance and R_{o1} is the resistance caused by the ripple current of L. At a steady state, the instantaneous equivalent circuit of the 1st block is expressed by Fig. 4, where R_{on} is the on-resistance of S_1, R_l is the internal resistance of L, $\Delta q_{T_i,v_{in}}$ is the electric charge of the V_{in} in State-T_i, ($i = 1$, 2), and $\Delta q_{T_i,v_o}$ is the electric charge of the output terminal V_o in State-T_i. Since the electric charges of C_1 are the same at the start and end of the cycle T, the differential value Δq^1_{Ti} satisfies

$$\Delta q^k_{T_1} + \Delta q^k_{T_2} = 0, \quad \text{where} \quad T = T_1 + T_2, T_1 = DT, \quad \text{and} \quad T_2 = (1-D)\,T. \tag{3}$$

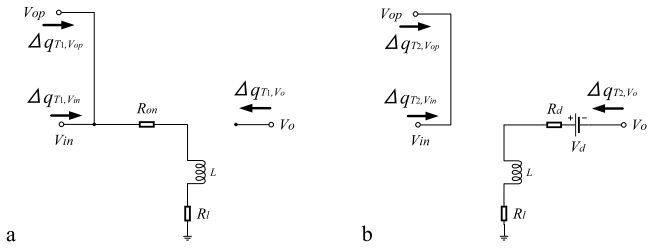

Fig. 4. Instantaneous equivalent circuit of the 1st block: (a) state-T_1; (b) state-T_2.

Based on the Kirchhoff's current law, the differential values of the inductor current Δi_L are expressed as

$$\Delta i_{L,T_1}(t) = \left(\frac{\Delta i_L}{T_1}\right) t + \left(I_{in} - \frac{\Delta i_L}{2}\right) \quad \text{and} \quad \Delta i_{L,T_2}(t) = -\left(\frac{\Delta i_L}{T_2}\right) t + a_1, \tag{4}$$

where $\Delta i_{L,T_1}(t)$ ($\subseteq [0, T_1)$) is the differential values of the inductor current in State-T_1, $\Delta i_{L,T_2}(t)$ ($\subseteq [T_1, T_2]$) is the differential values of the inductor current in State-T_2, I_{in} is the average input current, and a_1 is a parameter. In a steady state, $\Delta i_{L,T_1}(t)$ is equal to $\Delta i_{L,T_2}(t)$. Therefore, the parameter a_1 is obtained as

$$a_1 = I_{in} + \left\{\frac{1+D}{2(1-D)}\right\} \Delta i_L. \tag{5}$$

From Eqs. (4) and (5), Δi_L is given by

$$\Delta i_L = \Delta i_{L,T_1}(T_1) - \Delta i_{L,T_1}(0) = \frac{1}{L}\int_0^{T_1} V_{in} dt = \frac{V_{in}}{L} T_1 \tag{6}$$

$$\text{and} \quad -\Delta i_L = \Delta i_{L,T_2}(T) - \Delta i_{L,T_2}(T_1) = \frac{1}{L}\int_{T_1}^{T} V_o dt = \frac{V_o}{L} T_2. \tag{7}$$

From Eqs. (6) and (7), we have

$$V_o = m_1 V_{in} \quad \text{and} \quad I_o = \frac{1}{m_1} I_{in}, \quad \text{where} \quad m_1 = -\left(\frac{D}{1-D}\right). \tag{8}$$

Here, the total consumed energy, W_T, of Fig. 3 is expressed as

$$W_T = W_{T_1} + W_{T_2}, \tag{9}$$

$$\text{where} \quad W_{T_1} = \int_0^{T_1} (R_{on} + R_l) \left(\Delta i_{L,T_1}(t)\right)^2 dt \quad \text{and} \quad W_{T_2} = \int_{T_1}^{T} (R_d + R_l) \left(\Delta i_{L,T_2}(t)\right)^2 dt$$

Eq. (11) can be rewritten as

$$W_T = m_1^2 \{D(R_{on} + R_l) + (1-D)(R_d + R_l)\} T (I_o)^2 + \frac{1}{12} \{D(R_{on} + R_l) + (1-D)(R_d + R_l)\} T (\Delta i_L)^2,$$

$$\text{where} \quad \Delta i_L = \frac{V_{in}}{L} T_1 = \left(\frac{I_o R_{L1}}{m_1 L}\right) DT. \tag{10}$$

In Eq. (10), R_{L1} denotes the output load of the 1st block. In Fig. 3, W_T is expressed as

$$W_T = (R_{ac} + R_{o1}) (I_o)^2 T. \tag{11}$$

Therefore, we have

$$R_{o1} = m_1^2 \{D(R_{on} + R_l) + (1-D)(R_d + R_l)\} \quad \text{and} \quad R_{ac} = \frac{R_{o1}}{3} \left(\frac{DT R_{L1}}{2 m_1^2 L}\right)^2. \tag{12}$$

Therefore, the equivalent circuit of the 1st block is obtained from Eq. (12).

Next, the equivalent circuit of the 2nd block is analyzed by using Fig. 5. At a steady state, the relation between $\Delta q_{T_i}^k$'s ($k = 1, 2, out$) is obtained by using the Kirchhoff's current law as follows:

$$\Delta q_{T_1, v_{i2}} = \Delta q_{T_1}^1 + \Delta q_{T_1}^2 \quad \text{and} \quad \Delta q_{T_2, v_{i2}} = -\Delta q_{T_2}^1 + \Delta q_{T_2}^2, \tag{13}$$

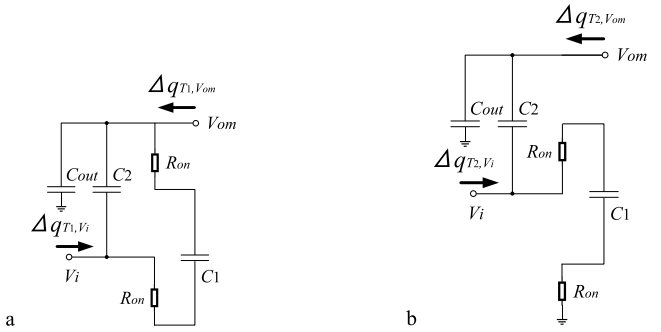

Fig. 5. Instantaneous equivalent circuit of the 2nd block: (a) state-T_1; (b) state-T_2.

$$\Delta q_{T_1,v_{o2}} = -\Delta q_{T_1}^{out} - \Delta q_{T_1}^{1} - \Delta q_{T_1}^{2} \quad \text{and} \quad \Delta q_{T_2,v_{o2}} = -\Delta q_{T_2}^{out} - \Delta q_{T_2}^{2}. \tag{14}$$

Since the average input/output currents, I_{i2} and I_{o2} $(= I_{out})$, is expressed as

$$I_{i2} = \frac{\Delta q_{v_{i2}}}{T} = \frac{\Delta q_{T_1,v_{i2}} + \Delta q_{T_2,v_{i2}}}{T} \quad \text{and} \quad I_{o2} = \frac{\Delta q_{v_{o2}}}{T} = \frac{\Delta q_{T_1,v_{o2}} + \Delta q_{T_2,v_{o2}}}{T}, \tag{15}$$

We have the relation between the input and the output from Eqs. (13)–(15) as follows:

$$\Delta q_{V_{i2}} = -2\Delta q_{V_{out}} \quad \text{and} \quad I_{i2} = -2I_{o2}. \tag{16}$$

In the same way, the total consumed energy, W_T, of the 2nd block is discussed as follows:

$$W_T = W_{T_1} + W_{T_2}, \quad \text{where} \quad W_{T_1} = 2R_{on}\frac{\left(\Delta q_{T_1}^{1}\right)^2}{T_1} \quad \text{and} \quad W_{T_2} = 2R_{on}\frac{\left(\Delta q_{T_2}^{1}\right)^2}{T_2}. \tag{17}$$

Eq. (17) can be rewritten as

$$W_T = \frac{2R_{on}}{D\,(1-D)}\frac{\left(\Delta q_{v_{o2}}\right)^2}{T}. \tag{18}$$

Therefore, we have

$$R_{SC2} = \frac{2R_{on}}{D\,(1-D)}, \tag{19}$$

Because W_T of Fig. 3 can be expressed as

$$W_T = R_{SC2}\frac{\left(\Delta q_{v_{o2}}\right)^2}{T}. \tag{20}$$

Finally, we obtain the equivalent circuit of the proposed converter as shown in Fig. 6. From Fig. 6, the output voltage and the power efficiency can be derived easily.

4. Performance evaluation

Through SPICE simulations, the characteristics are compared between the proposed hybrid converter and the traditional buck–boost converter. Fig. 7 demonstrates the simulated output voltage, where we conducted the SPICE

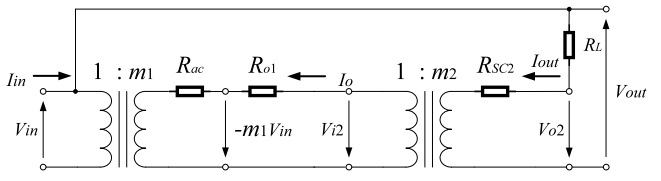

Fig. 6. Equivalent circuit of the proposed LED driver circuit.

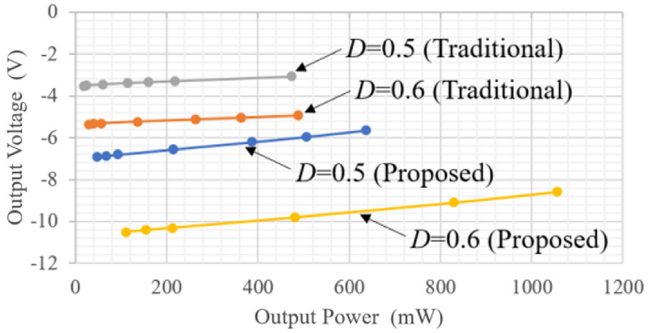

Fig. 7. Simulated output voltage as a function of time.

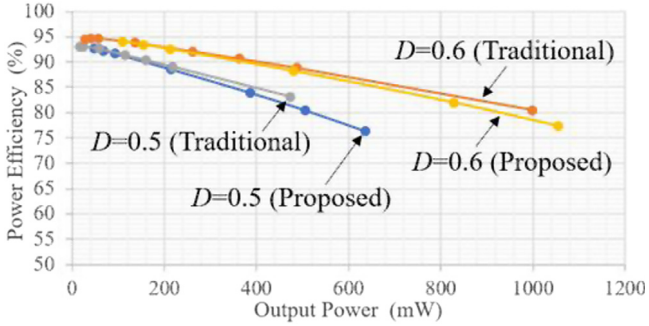

Fig. 8. Simulated output voltage as a function of time.

simulations under the conditions that $V_{in} = 3.7$ V, $L = 1$ mH, $C_1 = C_2 = C_{out} = 10$ μF, and $T = 10$ μs. As Fig. 7 shows, the proposed hybrid converter can provide higher output voltage than the traditional buck–boost converter. Fig. 8 depicts the simulated power efficiency. As you can see from Fig. 8, the power efficiency of the proposed hybrid converter is slightly lower than that of the traditional buck–boost converter if these converters are operated in the same D. Due to the internal resistance of the 2nd block, the power efficiency slightly decreases in the proposed hybrid converter. However, the proposed hybrid converter can achieve about 89% power efficiency and -10 V output when the parameter D is 0.6 and the output load is 400 mW.

5. Experiments

To confirm the feasibility of the proposed hybrid buck–boost converter, the breadboard circuit was built with commercially available ICs, namely, photo MOS relays AQW 217, darlington sink driver TD 62004 APG, a microcontroller PIC, and a diode 1N 4007. The experiments were conducted under the conditions that $V_{in} = 3.7$ V, $L = 100$ mH, $C_1 = C_2 = C_{out} = 10$ μF, $T = 10$ ms, and the output load $R_L = 51$ kΩ. Fig. 9 demonstrates the experimental results of the proposed hybrid converter. As Fig. 9 shows, the voltage gain of the proposed hybrid converter can be controlled by the parameter D. In Fig. 9(a) and (b), the outputs -6.38 V and -9.62 V were measured against the duty cycles $D = 0.5$ and $D = 0.6$, respectively. As you can see from these results and Eq. (1), the proposed converter can achieve higher voltage gain than that of the traditional buck–boost converter.

6. Conclusion

For LED lighting applications, a hybrid buck–boost dc–dc converter and its analysis method have been presented in this paper. First, in order to clarify the characteristics, the equivalent circuit was derived theoretically. In this theoretical analysis, the equivalent circuit was expressed as a four-terminal equivalent model. Next, through SPICE simulations, the performance was compared between the proposed hybrid converter and the traditional buck–boost converter. When the output load was 400 mW, about 89% power efficiency and -10 V output were achieved in

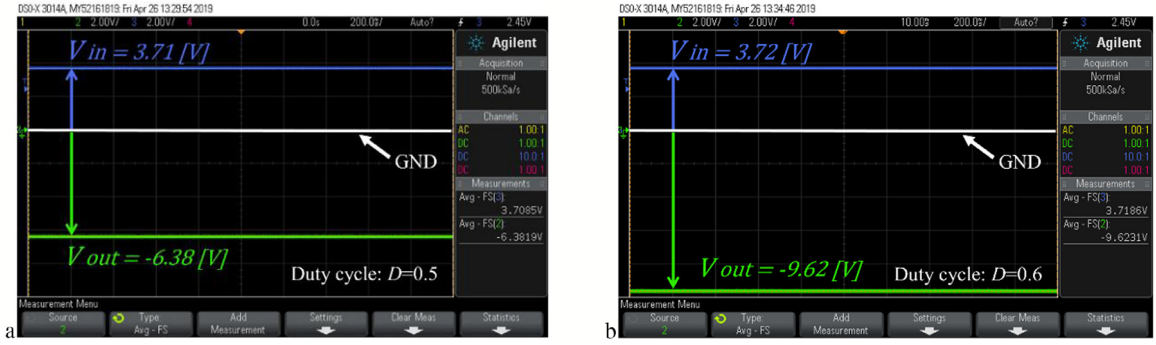

Fig. 9. Measured output voltages of the proposed hybrid converter: (a) $D = 0.5$; (b) $D = 0.6$.

the proposed hybrid converter. Furthermore, the proposed hybrid converter demonstrated higher voltage gain than the traditional buck–boost converter. Finally, the feasibility of the proposed hybrid converter was confirmed by breadboard experiments. The IC implementation of the proposed LED driver circuit is left to a future study.

References

[1] Eguchi Kei, Pongswatd Sawai, Watanabe Toshiya, Pannil Pittaya, Tirasesth Kitti, Sasaki Hirofumi. A white LED driver using a buck-boost converter. IEEJ Trans Electr Electron Eng 2010;5(5):613–4.

[2] Zebraoui Otmane, Bouzi Mostafa. Robust sliding mode control based MPPT for a PV/wind hybrid energy system. Int J Intell Eng Syst 2018;11(5):290–300.

[3] Menke F Maikel, Seidel Álysson R, Tambara Rodrigo V. LLC LED driver small-signal modeling and digital control design for active ripple compensation. IEEE Trans Ind Electron 2019;66(1):387–96.

[4] Eguchi Kei, Pongswatd Sawai, Asadi Farzin, Fujisaki Haruka. A high voltage gain SC DC-DC converter based on cross-connected Fibonacci-type converter. In: Proc. 2018 international conference on engineering, applied sciences, and technology; 2018. p. 1–4.

[5] Gao Yuan, Li Lisong, Mok KT Philip. Design of LED driver ICs for high-performance miniaturized lighting systems. In: Proc. 2018 IEEE 30th international symposium on power semiconductor devices and ICs; 2018. p. 508–11.

[6] Eguchi Kei, Julsereewong Prasit, Julsereewong Amphawan, Fujimoto Kuniaki, Sasaki Hirofumi. A Dickson-type adder/subtractor DC-DC converter realizing step-up/step-down conversion. Int J Innovative Comput Inf Control 2013;9(1):123–38.

[7] Ma Jianguang, Wei Xueye, Hu Liang, Zhang Junhong. LED driver based on boost circuit and LLC converter. IEEE Access 2018;6:49588–600.

[8] McRae Tim, Prodić Aleksandar, Chakraborty Sombuddha, McIntyre William, Aguilar Alvaro. A multi-output hybrid divided power converter for LED lighting applications. In: proc. 2018 IEEE 19th workshop on control and modeling for power electronics; 2018. p. 1–7.

[9] Abe Kanji, Smerpitak Krit, Pongswatd Sawai, Oota Ichirou, Eguchi Kei. A step-down switched-capacitor AC–DC converter with double conversion topology. Int J Innov Comput Inf Control 2017;13(1):319–30.

[10] Eguchi Kei, Junsing Tipparat, Julsereewong Amphawan, Do Wanglok, Oota Ichirou. Design of a nesting-type switched-capacitor AC/DC converter using voltage equalizers. Int J Innovative Comput Inf Control 2017;13(4):1369–84.